Available online at www.sciencedirect.com

SciVerse ScienceDirect

Ceramics International 39 (2013) 2699–2707

CERAMICS INTERNATIONAL

www.elsevier.com/locate/ceramint

Optical and photoelectrochemical properties of a TiO_2 thin film doped with a ruthenium–tungsten bimetallic complex

Khuzaimah Arifin[a,b], Wan Ramli Wan Daud[a,b], Mohammad B. Kassim[a,c,*]

[a]*Fuel Cell Institute, Universiti Kebangsaan Malaysia, 43600 UKM Bangi, Selangor, Malaysia*

[b]*Department of Chemical and Process Engineering, Universiti Kebangsaan Malaysia, 43600 UKM Bangi, Selangor, Malaysia*

[c]*School of Chemical Sciences and Food Technology, Faculty of Science and Technology Universiti Kebangsaan Malaysia, 43600 UKM Bangi, Selangor, Malaysia*

Received 29 June 2012; received in revised form 2 September 2012; accepted 13 September 2012
Available online 7 October 2012

Abstract

Optical and photoelectrochemical (PEC) properties of a TiO_2 thin film electrode doped with a new variation of ruthenium–(4,4′dimethyl-2,2′-bipyridine)–isothiocyanato–tungsten[bis-(phenyl-1,2-ethilenodithiolenic)] bimetallic complex (BM) were investigated. Physical adsorption process was used to immobilise the BM on the TiO_2 thin film. Crystalline structure and surface morphology of the thin films were examined using scanning electron microscopy (SEM), X-ray diffraction (XRD) and energy-dispersive X-ray (EDX) techniques. N3 commercial dye was also used as a dopant to the TiO_2 films for comparison. Light absorption spectra and bandgap energy of the thin films were determined using UV–vis spectroscopy. Light absorption of the TiO_2 thin film doped with BM was better than the TiO_2 doped with the N3 commercial dye. Band edges of the TiO_2 thin film and the BM were determined via cyclic voltammetry (CV) measurements. Top-edge of the BM valence band (VB) was more positive than the bottom edge of the conduction band (CB) of the TiO_2 film (vs. NHE). PEC analysis indicated that photocurrent of TiO_2 doped with the BM electrode was higher than TiO_2 doped with the N3 in the beginning of illumination process, but the performance was defeated after a while. Based on the optical properties and the PEC analyses, BM has potential to be used as dye sensitisers for a PEC cell.

Keywords: Optical properties; TiO_2; Electrode; Dye-sensitiser

1. Introduction

Hydrogen has been considered as an alternative fuel source to replace fossil fuels for many years [1,2], and has been used in fuel cells to generate electricity where the only by-product is water [3]. A green method for producing hydrogen is through the photoelectrolysis of water using a semiconductor photoelectrode. In 1972, Fujishima and Honda demonstrated the photoelectrolysis of water molecules using the *n*-type TiO_2 semiconductor and platinum (Pt) electrodes [4,5]. However, the efficiency of this process was low because TiO_2 has a large bandgap that prevents it from adsorbing visible light, which accounts for 50% of solar radiation, thereby limiting its application to the UV region of the solar spectrum [6]. The bandgap measures the separation of the VB and CB in a material, which determines photon absorption and charge migration. When the photon energy from irradiation is greater than the bandgap energy, some electrons are excited from the VB to CB and leave holes in the VB (Eq. (1)). Photo-generated electrons and holes travel to the semiconductor surface where oxidation (O_2) (Eq. (2)) and reduction (H_2) (Eq. (3)) reactions occur [7].

$$2h\nu \rightarrow 2e^- + 2h^{\bullet} \quad (1)$$

$$2h^{\bullet} + H_2O_{(l)} \rightarrow \tfrac{1}{2}O_{2(g)} + 2H^+ \quad (2)$$

$$H^+ + 2e^- \rightarrow H_{2(g)} \quad (3)$$

For the water-splitting reaction to occur, the top-edge position of the semiconductor's VB should be more positive than the oxidation potential of H_2O to O_2 ($E_{O_2H_2O} = 1.23$ eV vs. NHE at pH = 0), and the bottom

*Corresponding author. Tel.: +60 3 89216045; fax: +60 3 89216024.
E-mail address: mbkassim@ukm.my (M.B. Kassim).

0272-8842/$ - see front matter © 2012 Elsevier Ltd and Techna Group S.r.l. All rights reserved.
http://dx.doi.org/10.1016/j.ceramint.2012.09.037

Table 1
Main PEC water-splitting requirements [8].

Condition	Requirement
PEC water-splitting	$H_2O_{(liquid)} + 2\ hv \rightarrow \frac{1}{2}O_{2(gas)} + H_{2(gas)}$
Minimum potential	$E^0{}_{H_2O}(25\ ^\circ C)_{min} = 1.229$ eV
Practical potential (+overpotential and losses)	$E^0{}_{H_2O}(25\ ^\circ C)_{prac} = 1.6-2.0$ eV $E_{bandgap} > E^0{}_{H_2O}$
Utilisation of sunlight	UV > hv (Vis) > IR $hv \geq E_{bandgap}$
Band edges	$C_{band\ edge} < E^0{}_{H_2H^+}$ $V_{band\ edge} > E^0{}_{O_2H_2O}$

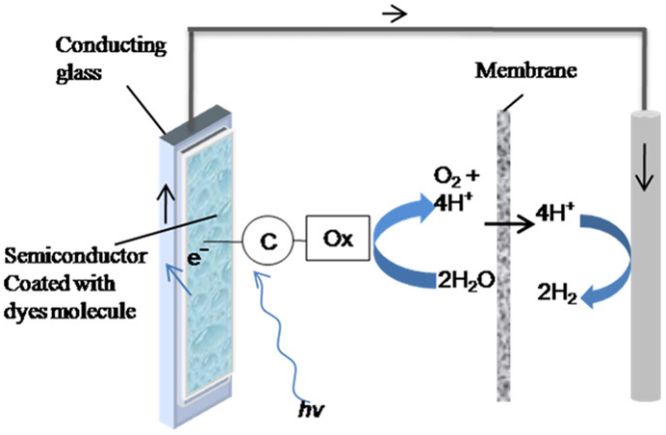

Fig. 1. Concept of dye-sensitised PEC water-splitting cell [16].

edge of the CB should be more negative than the reduction potential of H^+ to H_2 ($E_{H^+}H_2 = 0$ eV vs. NHE at pH = 0) [7,8]. Several requirements that should be fulfilled for the PEC water splitting to occur are shown in Table 1 [8].

Intensive research has been conducted to reduce the semiconductor's bandgap to expand the adsorption spectrum to wider wavelengths, including the use of a dye-sensitised PEC cell [9]. In this paper, the optical and PEC properties of a TiO_2 thin film doped with a new variation of bimetallic complex are presented. The bimetallic complex, called ruthenium–(4,4′dimethyl-2,2′-bipyridine)–isothiocyanato–tungsten[bis-(phenyl-1,2-ethilenodithiolenic)], abbreviated as BM, has unique properties including multicentred redox activity, and has a higher molar extinction coefficient for electronic absorption compared to the cis–bis(iso-thiocyanato) bis(2,2′-bipyridyl-4,4′-di-carboxylato) ruthenium(II) commercial dye, abbreviated as N3 [17].

The dye-sensitised PEC cell for water-splitting mimics photosystem II of natural photosynthesis, where the complex molecule acts as dye-sensitiser for light harnessing, as shown in Fig. 1 [10]. The ruthenium bipyridyl monometallic transition metal complex is commonly used as a dye-sensitiser, and its use has been shown to increase the efficiency of solar cells up to 11.4% [11,12]. However, the monometallic complex sensitiser has limitations for the transfer of electrons, which limits the performance of the dye-sensitised PEC cell. One strategy to increase the efficiency is to use a bimetallic complex as a dye sensitiser. The intramolecular energy transfer in a bimetallic complex is expected to provide more electrons to the photoelectrode, which inhibits charge recombination in the UV-excited TiO_2 thin film and extends the lifetime and light absorption range of the PEC water-splitting cell [13–16]. Investigating the optical properties is a simple method for determining the effect of intramolecular energy transfer in a bimetallic complex on the donation of electrons to the photoelectrode.

2. Materials and methods

The TiO_2 electrodes were prepared using commercial colloidal TiO_2 powder (Degussa P25, average size of 10–50 nm) by doctor-blading onto fluorine-doped tin oxide (FTO) glass plates. The FTO slides were sequentially sonicated for 15 min in water, ethanol, acetone, and then analytical grade ethanol. The TiO_2 powder (0.5 g) was ground in water (1 ml) containing acetylacetone (0.1 ml) to produce a viscous paste. The paste was then formed through a very slow addition of water (1.7 ml) and one drop of Triton X-100 [18]. Afterwards, the paste was smeared onto a clean FTO slide that was immobilised by an adhesive strip tape, which was also used to determine the film thickness. The film was dried at room temperature for 60 min followed by heating at 150 °C for 15 min, and it was then annealed at 450 °C for 30 min. Field Emission Scanning Electron Microscopy (FESEM) analysis using a Carl Zeiss SUPRA 55VP was performed to determine the film thickness and surface morphology, and a Bruker D8-Advance diffractometer (XRD) was used to determine the crystallinity and structure of the TiO_2 thin film.

BM was synthesised following the synthetic scheme shown in Fig. 2 and was used as a dye sensitiser onto a TiO_2 thin film [17]. BM (IV) was synthesised from a condensation reaction of a tungsten dithiolene carbonyl complex, $[W(S_2C_2Ph_2)_2(CO)_2]$ (II), with ruthenium–[bis(4,4′-dimethyl-2,2′-bipyridyl)–isothiocyanato], abbreviated as $[Ru(dmtbpy)_2NCS_2]$ complex (III). The starting ruthenium bipyridyl complex $[Ru(dmtbpy)_2NCS_2]$ was prepared from the reaction of 4,4′-dimetyl-2,2′-bipyridine with dichloro(*p*-cymene)ruthenium(II) dimer and NH_4NCS. Meanwhile, the $[W(S_2C_2Ph_2)_2(CO)_2]$ complex was prepared via the reaction of the photo-generated $W(CO)_5THF$ intermediate with a thioester. The products were characterised using FTIR, ^1H and ^{13}C NMR and UV–vis spectroscopies using a Thermo Nicolet 6700 FTIR spectrometer, Bruker Avance 400 MHz spectrometer and a Lambda 35 UV/Vis spectrophotometer, respectively. Additionally, a micro-elemental analysis was performed using an Elemental Micro

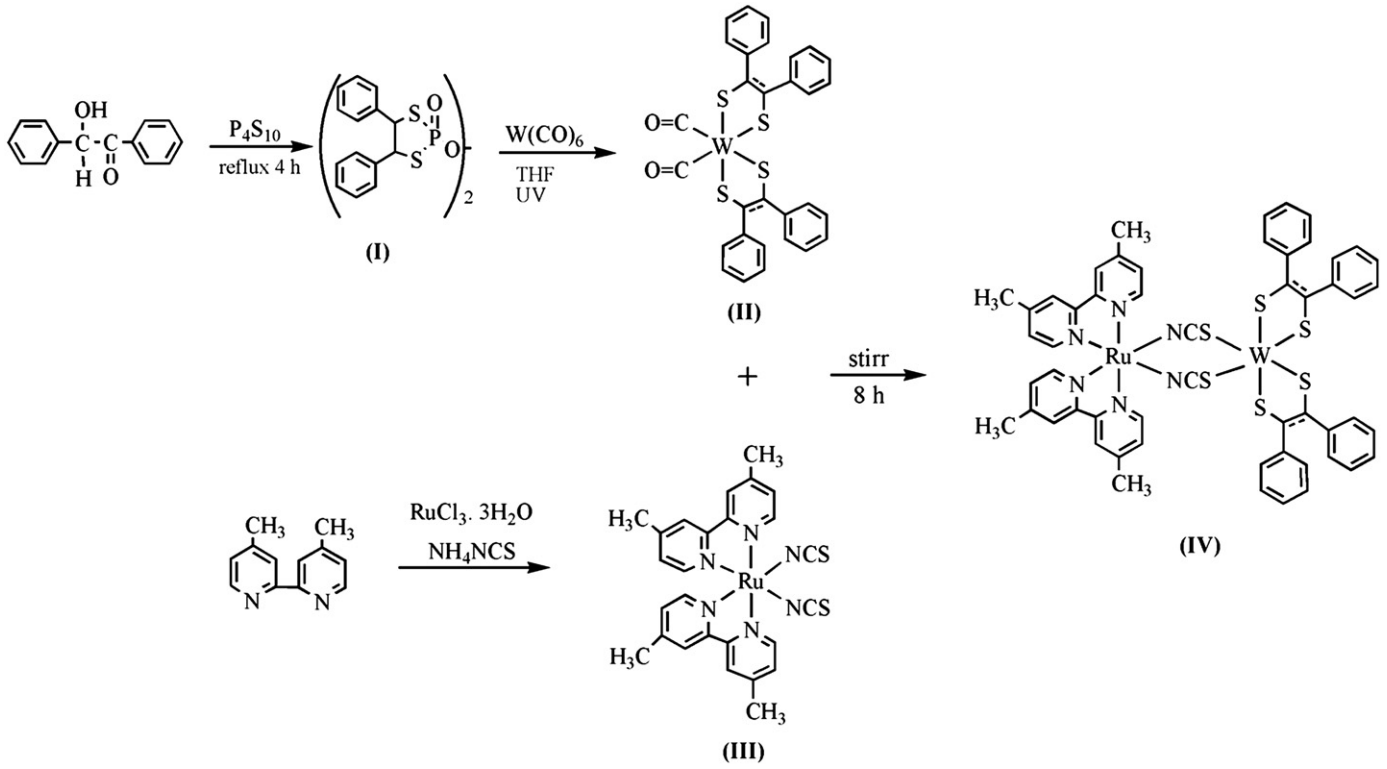

Fig. 2. Reagents and synthesis scheme for BM.

Cube CHNS analyser. The BM is a dark brown solid that is soluble in polar aprotic solvents, such as DMF and DMSO, but is not soluble in non-polar solvents, including THF and dichloromethane.

The dye adsorption process involved immersing a TiO_2 electrode in 1 M of BM in DMF solvent for 24 h at room temperature in a dark room. The same procedure was used to adsorb $Ru(dcbpy)_2(NCS)_2$ (N3 dye, Solaronix). The electrodes were then dried in a desiccator cabinet at room temperature for 48 h. EDX analyses were performed using an Oxford electron microprobe, which was attached to the SEM to confirm the presence of ruthenium and tungsten metals in the BM molecule on the TiO_2 film. A Perkin–Elmer Lambda 35 UV/Vis spectrophotometer was used to measure the optical transmission spectra of the electrodes in the wavelength range from 200 nm to 1000 nm.

The optical bandgap energy of the TiO_2 thin film was calculated using the following equations:

$$\alpha = \left[\frac{B(h\upsilon - E_g)^p}{h\upsilon}\right] \quad (4)$$

and

$$\alpha = \left[\frac{1}{d}\ln\left(\frac{1}{T}\right)\right] \quad (5)$$

where α, B, d and T are the absorption coefficient, a constant, the thickness of the film (cm) and a normalised transmittance, respectively. The bandgap (E_g) of a thin film can be determined by plotting the photon energy ($h\upsilon$) *vs.* $\alpha h\upsilon$ at various wavelengths [19].

The energy of the ground and excited states of the BM were determined using CV analysis, which was performed using an electrochemical cell with three electrode systems: a platinum disk, a platinum wire, and a Ag/AgCl were used as the working, auxiliary, and reference electrodes, respectively. The redox potentials of the BM (0.1 mM) were determined in DMF that contained 0.1 M of tetrabutylammonium hexaflorophosphate ($TBAPF_6$) electrolyte in a nitrogen atmosphere at room temperature. The redox potentials of the TiO_2 thin film were determined by constructing the TiO_2 film working electrode.

A similar setup was used for the PEC analysis. The TiO_2 thin film was used as the working photoelectrode. There were three photoelectrodes used in this study, which consisted of an undoped TiO_2 film and TiO_2 doped with BM and N3. The current density measurement was conducted in triple-distilled water that contained 5% sodium sulphate (0.5 M) as the electrolyte. Current density on the surface of the TiO_2 electrodes was measured in the dark and under illumination using a 400-watt xenon lamp at a distance of 1 m from the PEC cell as a light source [20]. The changes in the current during irradiation were monitored and recorded.

3. Results and discussion

3.1. Characterisation of the photoelectrode

The performance of a PEC cell is affected by several aspects of the TiO_2 thin films, including the crystalline

phase, particle size, pore size and thickness of the films [21–25]. Generally, TiO_2 has three crystal phases, anatase, rutile and brookite, with bandgaps of 3.2, 3.0 and 3.4 eV, respectively. The XRD patterns of the TiO_2 thin films produced in this study indicate the presence of the anatase and rutile phases, with compositions of 69.27% and 14.91%, respectively (Fig. 3). The qualitative crystal size of the TiO_2 anatase and rutile phases determined from the FESEM images ranges from 26.8 to 41.3 nm, while the pore sizes of the thin films ranged from 44.0–130.3 nm. The film thickness was approximately 2 μm (Fig. 4). A previous study by Park et al. [27] demonstrated that the most efficient thickness of a photoelectrode is approximately 2–3 μm [26–28]. After preparation and characterisation, the thin films were then immersed in solution containing 1 M of each BM and N3 respectively with the same methods and solvents.

EDX was used to determine the presence of the dopant element in the photoelectrode. Fig.5 shows the EDX analysis of the TiO_2 thin film electrode doped with BM and N3, where all elements of BM and N3 are present in each photoelectrode. The amount of tungsten and ruthenium on the TiO_2 films doped with BM were approximately (wt%) 0.12% and 0.10%, respectively, while the amount of ruthenium on the TiO_2 films doped with N3 was about 0.25%. Total amount of metal elements from dope material on both electrodes were comparable.

3.2. Optical properties

Fig. 6 shows the light absorption spectrum of the three kinds of TiO_2 electrodes, in which the light absorption spectrum of electrode doped with BM was the highest compared to the undoped and the TiO_2 photoelectrode

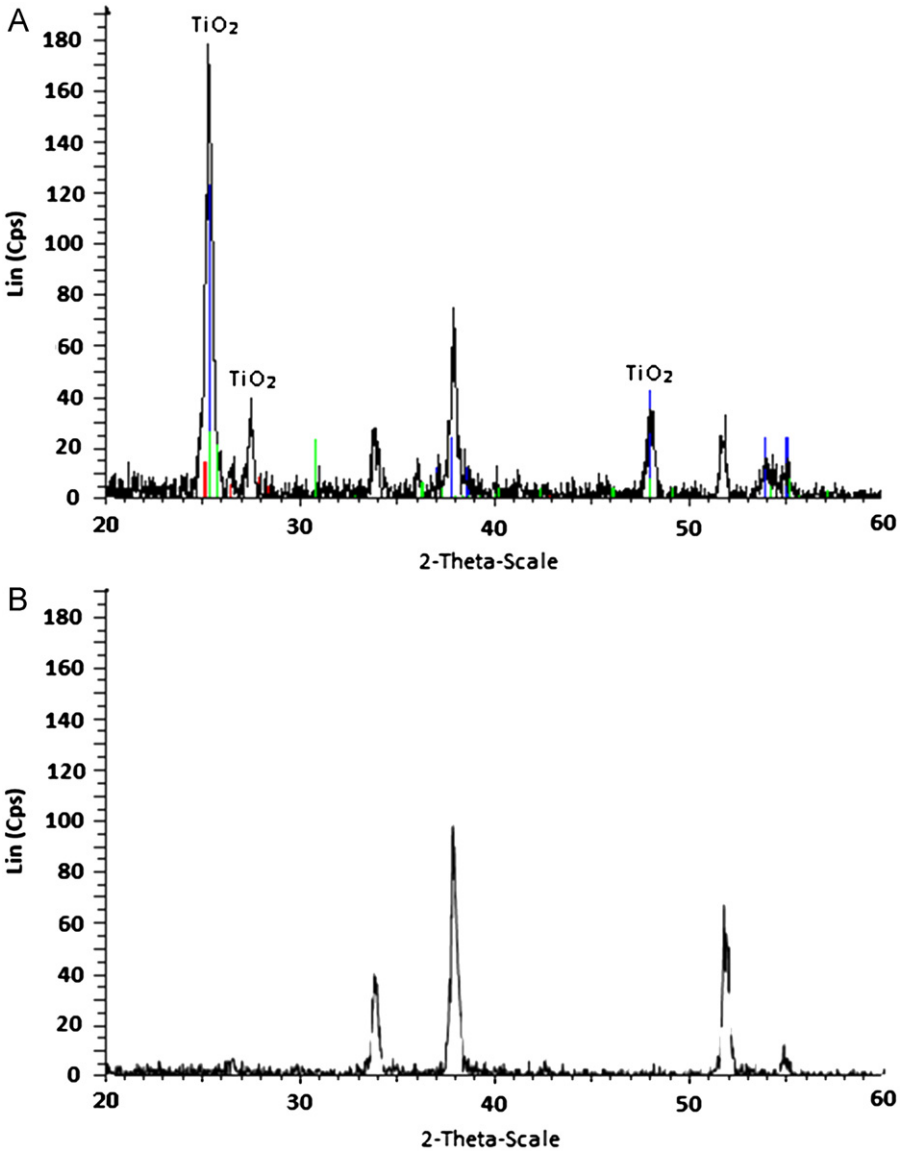

Fig. 3. XRD pattern of the TiO_2 on FTO (A) and a FTO blank (B).

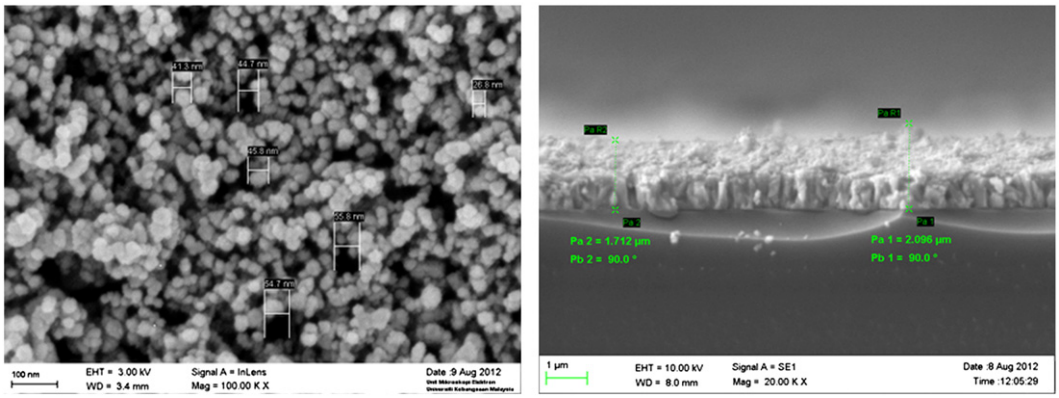

Fig. 4. Surface morphology of the TiO_2 thin film electrode from SEM analysis.

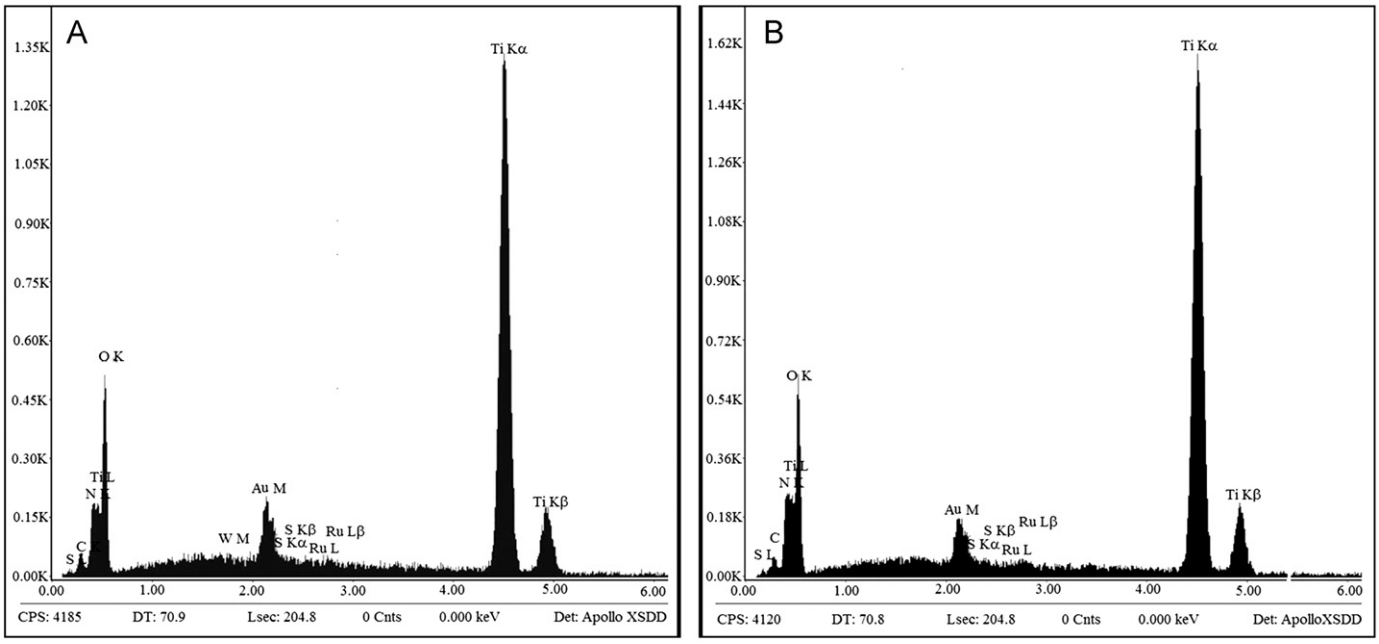

Fig. 5. EDX elemental analysis of the TiO_2 thin film electrode: (A) The elemental spectrum of the TiO_2 thin films doped with BM and (B) the elemental spectrum of the TiO_2 thin films doped with N3.

doped with the N3 dye. The TiO_2 electrode doped with BM also exhibits a sharp peak at approximately 450 nm, and the origin of this absorption peak is uncertain but may be related to the dopant. The N3-doped TiO_2 also exhibits a similar behaviour, although it occurs with a lower intensity. The UV–vis adsorption data were used to determine the bandgaps of the photoelectrodes. Using Eq. (4) and (5), where the film thickness was 2 µm (SEM analysis), the bandgap was determined by plotting αhv and the photon energy (hv) at various wavelengths (Fig. 7). The plot indicates that the bandgap of the undoped TiO_2 was 3.12 eV, which is highly proper for an electrode with a mixture of the anatase and rutile phases. Furthermore, the bandgap energy for the TiO_2 sensitised with N3 and BM were 3.02 eV and 2.97 eV, respectively. Doping reduces the TiO_2 electrode bandgap, and it was shown that BM produced a better photo-absorption range compared to the N3 dye.

3.3. Calculation of the band edges

For a dye molecule to inject an electron into the photoelectrode semiconductor, the bottom edge of the CB of the dye molecule should be more negative than the bottom edge of the CB of the semiconductor (vs. NHE) [29]. The energy levels were determined using Eqs. (6) and (7):

$$E^0_{D^+/D^*} = E^0_{D^+/D} + E_g \quad (6)$$

and

$$E_g\,(\mathrm{eV}) = 1240/_{g}(\mathrm{nm}) \quad (7)$$

where $E^0_{D^+/D^*}$ and $E^0_{D^+/D}$ are the energy in the excited and the ground states, respectively. The ground state energy, $E^0_{D^+/D}$, is calculated based on the cyclic voltammetry analysis in dark conditions. E_g and λ_g are the bandgap

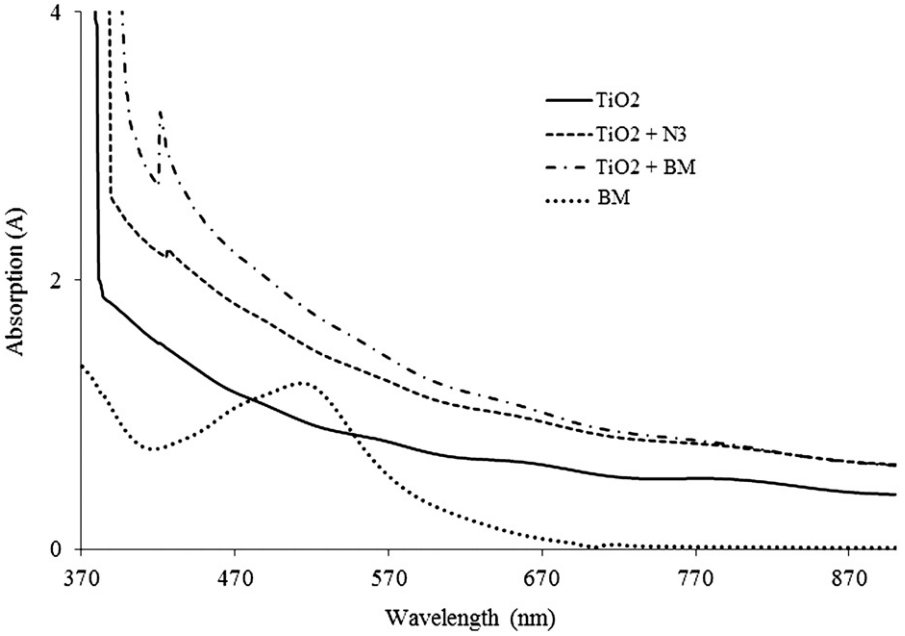

Fig. 6. Absorption spectra of the undoped and doped TiO_2 films with N3 dye and BM.

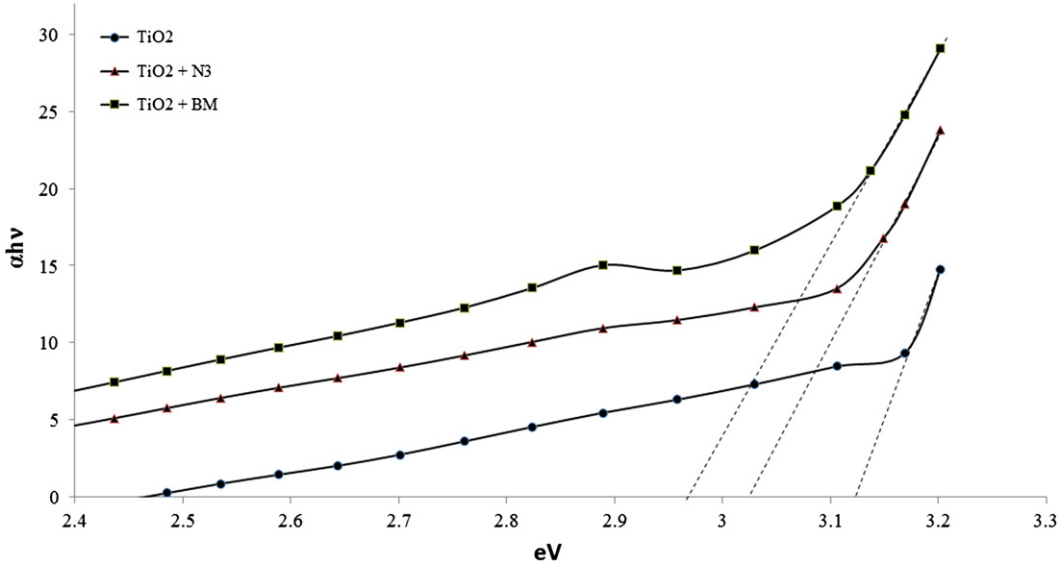

Fig. 7. Bandgap determination for the TiO_2 film and the TiO_2 films doped with the N3 dye and BM.

energy and the absorption wavelength threshold of the doping material, respectively.

Based on the cyclic voltammetry analysis of the BM in Fig. 8, the redox equilibrium point was observed at 0.0 V (vs. Ag/AgCl), which was equivalent to 0.004 eV (vs. SCE) and −4.75 eV (vs. vacuum). The absorption wavelength threshold of the BM was 700 nm (Fig. 6). Using Eq. (7), the Eg for the BM was determined to be 1.77 eV, thus the excited state energy was −2.98 eV (vs. vacuum). The same method was also used to determine the energy of the excited state of the TiO_2 electrode, where the TiO_2 undoped equilibrium point was observed at 0.06 V (vs. Ag/AgCl), which was equivalent to 2.94 eV (vs. NHE) and −7.47 eV (vs. vacuum). Furthermore, the excited state of TiO_2 was observed at −4.35 eV (vs. vacuum). Fig. 9 shows the position of the band edges, in which the BM had a more negative CB bottom edge than the TiO_2 electrode.

3.4. Photoelectrochemical analysis

PEC analyses were performed by measuring current density of the electrode under various incident photo-energy. The photocurrent values were obtained from the difference in currents measured in the dark and under irradiation. Current density of the TiO_2 electrode with and without doping against a bias voltage is shown in Fig. 10.

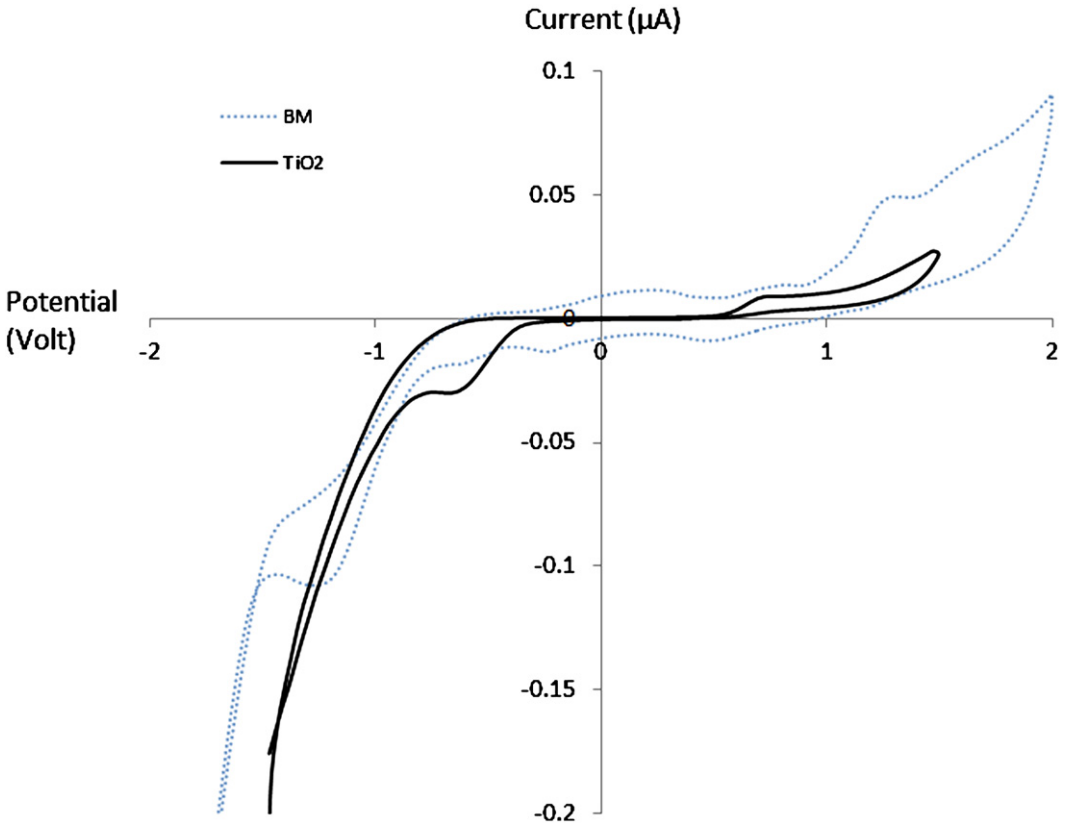

Fig. 8. Cyclic voltammogram of the BM molecule and the TiO_2 thin film (scan rate=0.1 Vs^{-1}) vs. Ag/AgCl.

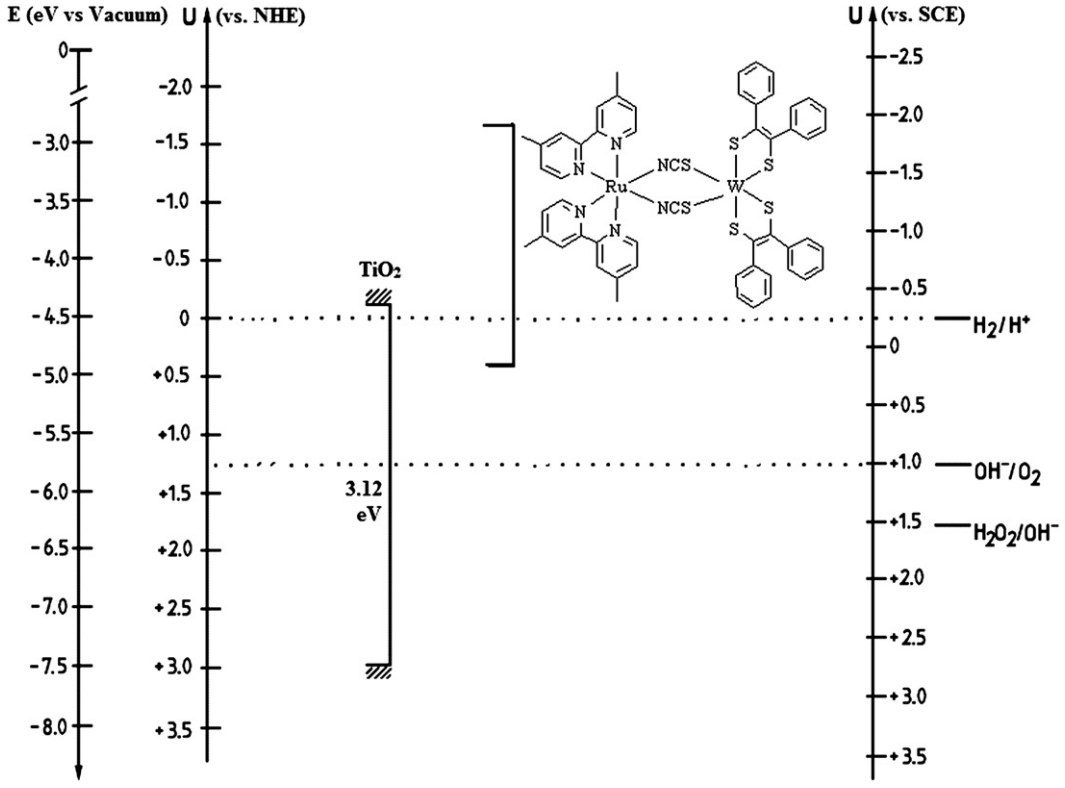

Fig. 9. Energy level diagram of the TiO_2 electrode and BM molecule.

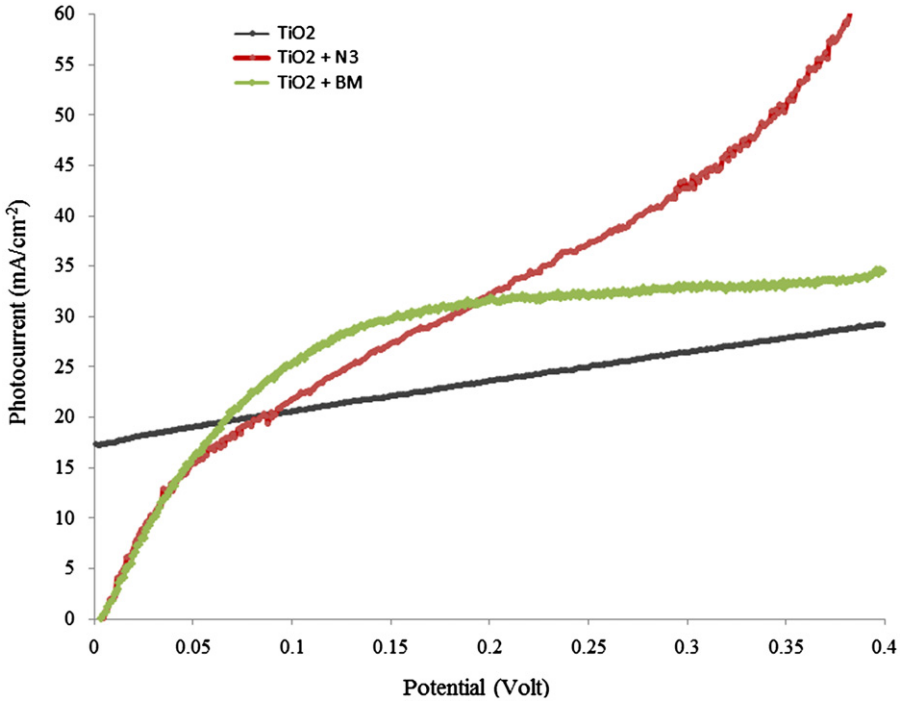

Fig. 10. Light and dark current density of the TiO_2 photoelectrode doped with the photosensitiser molecule.

Current of the three types of TiO_2 photoelectrodes under light was higher than the dark current. At the lowest applied voltage stage, the current density generated by the TiO_2 electrode doped with BM was higher than the TiO_2 electrode sensitised by the N3 molecule and the TiO_2 electrode without doping. However, at the highest applied voltage, the current density of the TiO_2 electrode doped with the BM did not increase, whereas the current density of the TiO_2 electrode sensitised by the N3 dye increased linearly. This observation relates to the availability of anchoring groups on the doping material. The N3 dye was chemically adsorbed due to the availability of –COOH functional groups that facilitate chemical bonding, whereas the BM was physically adsorbed. Charge transfer from the physically adsorbed component was less effective than charge transfer from the chemically bonded N3 commercial dye [30]. Furthermore, there was an indication that the BM was leaching upon prolonged exposure to irradiation.

Although the photocurrent performance of the complex was lower compared to the N3 dye, the complex could still serve as a source of electrons that could be transferred to the TiO_2 electrode. Therefore, more research should be performed on BM, such as introducing an anchoring group (e.g., –COOH) to facilitate chemical bonding for more efficient charge transfer process from dye molecule to photoelectrode.

4. Conclusions

A new variation of heterobimetallic BM based on ruthenium and tungsten metals has been investigated for use as a dye sensitiser in wide-bandgap TiO_2 photoelectrodes. Analyses of the optical properties and the PEC analysis reveal that the BM is able to inject more electrons into the TiO_2 electrode. The bimetallic complex was immobilised on the TiO_2 film by physical absorption due to the absence of an anchoring group. Consequently, the PEC performance of TiO_2 doped with BM was still less than TiO_2 doped with the N3 dye. However, the performance of the TiO_2 doped with BM photoelectrode can still be increased by introducing anchoring groups to the bimetallic complex by converting the methyl group to a carboxyl group.

Acknowledgements

The authors would like to acknowledge the Universiti Kebangsaan Malaysia for sponsoring this project under UKM-GUP-07-30-190, UKM-AP-TK-08-2010 and UKM-OUP-TK-16/73 research grants.

References

[1] J. Nowotny, C.C. Sorrell, L.R. Sheppard, T. Bak, Solar–hydrogen: environmentally safe fuel for the future, International Journal of Hydrogen Energy 30 (2005) 521–544.
[2] M. Momirlan, T.N. Veziroglu, The properties of hydrogen as fuel tomorrow in sustainable energy system for a cleaner planet, International Journal of Hydrogen Energy 30 (2005) 795–802.
[3] T.N. Veziroglu, S. Sahın, 21st Century's energy: hydrogen energy system, Energy Conversion and Management 49 (2008) 1820–1831.
[4] A. Fujishima, K. Honda, Electrochemical photolysis of water at a semiconductor electrode, Nature 238 (1972) 37–38.
[5] M. Momirlan, L. Muresan, A.A.M. Sayigh, T.N. Veziroglu, The use of solar energy in hydrogen production, Renewable Energy 9 (1996) 1258–1261.
[6] H. Zweifel, R.D. Maier, M. Schiller, Plastics Additives Handbook, 6th ed., Carl Hanser Verlag, Munich, German, 2009.

[7] J. Zhu, M. Zäch, Nanostructured materials for photocatalytic hydrogen production, Current Opinion in Colloid and Interface Science 14 (2009) 260–269.
[8] L.J. Minggu, W.R. Wan Daud, M.B. Kassim, An overview of photocells and photoreactors for photoelectrochemical water splitting, International Journal of Hydrogen Energy 35 (2010) 5233–5244.
[9] R. Abe, K. Hara, K. Sayama, K. Domen, H. Arakawa, Steady hydrogen evolution from water on eosin Y-fixed TiO_2 photocatalyst using a silane-coupling reagent under visible light irradiation, Journal of Photochemistry and Photobiology A: Chemistry 137 (2000) 63–69.
[10] S.I. Allakhverdiev, V.D. Kreslavski, V. Thavasi, S.K. Zharmukhamedov, V.V. Klimov, S. Ramakrishna, H. Nishihara, M. Mimuro, R. Carpentier, T. Nagata, Photosynthetic energy conversion: hydrogen photoproduction by natural and biomimetic systems, in: A. Mukherjee (Ed.), Biomimetics Learning from Nature, InTech, Vukovar, Croatia, , 2010, p. 504.
[11] M. Grätzel, Dye-sensitized solar cells, Journal of Photochemistry and Photobiology C:Photochemistry Reviews 4 (2003) 145–153.
[12] L. Han, A. Islam, H. Chen, C. Malapaka, B. Chiranjeevi, S. Zhang, X. Yang, M. Yanagida, High-efficiency dye-sensitized solar cell with a novel co-adsorbent, Energy and Environmental Science 5 (2012) 6057–6060.
[13] R. Argazzi, E. Bertolasi, C. Chiorboli, C.A. Bignozzi, M.K. Itokazu, N.Y. Murakami Iha, Intramolecular energy transfer processes in binuclear Re–Os complexes, Inorganic Chemistry 40 (2001) 6885–6891.
[14] V. Balzani, F. Barigelletti, P. Belser, S. Bernhard, L.D. Cola, L. Flamigni, Rigid rodlike dinuclear Ru/Os complexes of a novel bridging ligand. Intercomponent energy and electron-transfer processes, The Journal of Physical Chemistry A 100 (1996) 16786–16788.
[15] C.J. Kleverlaan, M. Alebbi, R. Argazzi, C.A. Bignozzi, G.M. Hasselmann, G.J. Meyer, Molecular rectification by a bimetallic Ru–Os compound anchored to nanocrystalline TiO_2, Inorganic Chemistry 39 (2000) 1342–1343.
[16] K. Arifin, E.H. Majlan, W.R. Wan Daud, M.B. Kassim, Bimetallic complexes in artificial photosynthesis for hydrogen production: a review, International Journal of Hydrogen Energy 37 (2012) 3066–3087.
[17] K. Arifin, W.R.W. Daud, M.B. Kassim, A novel heterobinuclear complex based on ruthenium–tungsten metals in artificial photosynthesis technology, in: Proceedings of the 3rd International Conference on Fuel Cell and Hydrogen Technology, ICFCHT, Kuala Lumpur, Malaysia, 22 and 23 November, 2011.
[18] A.I. Kontos, I.M. Arabatzis, D.S. Tsoukleris, A.G. Kontos, M.C. Bernard, D.E. Petrakis, P. Falaras., Efficient photocatalysts by hydrothermal treatment of TiO_2, Catalysis Today 101 (2005) 275–281.
[19] M. Sreemany, S. Sen, A simple spectrophotometric method for determination of the optical constants and band gap energy of multiple layer TiO_2 thin films, Materials Chemistry and Physics 83 (2004) 169–177.
[20] A. Memar, W.R.W. Daud, S. Hosseini, E. Eftekhari, L.J. Minggu, Study on photocurrent of bilayers photoanodes using different combination of WO_3 and Fe_2O_3, Solar Energy 84 (2010) 1538–1544.
[21] A. Eshaghi, M. Pakshir, R. Mozaffarinia, Photoinduced properties of nanocrystalline TiO_2 sol–gel derived thin films, Bulletin of Materials Science 33 (2010) 365–369.
[22] Z. Yi, J. Liu, W. Wei, J. Wang, S.W. Lee, Photocatalytic performance and microstructure of thermal-sprayed nanostructured TiO_2 coatings, Ceramics International 34 (2008) 351–357.
[23] A. Eshaghi, R. Mozaffarinia, M. Pakshir, A. Eshaghi, Photocatalytic properties of TiO_2 sol–gel modified nanocomposite films, Ceramics International 37 (2011) 327–331.
[24] S. Pavasupree, Y. Suzuki, S. Pivsa-Art, S. Yoshikawa, Preparation and characterization of mesoporous MO_2 (M=Ti, Ce, Zr, and Hf) nanopowders by a modified sol–gel method, Ceramics International 31 (2005) 959–963.
[25] M.I. Badawy, M.Y. Ghaly, M.E.M. Ali, Photocatalytic hydrogen production over nanostructured mesoporous titania from olive mill wastewater, Desalination 267 (2011) 250–255.
[26] Y. Li, J. Hagen, W. Schaffrath, P. Otschik, D. Haarer, Titanium dioxide films for photovoltaic cells derived from a sol–gel process, Solar Energy Materials and Solar Cells 56 (1999) 167–174.
[27] N.G. Park, J.v.d. Lagemaat, A.J. Frank, Comparison of dye-sensitized rutile- and anatase-based TiO_2 solar cells, The Journal of Physical Chemistry B 104 (2000) 8989–8994.
[28] Q. Zhang, G. Cao, Nanostructured photoelectrodes for dye-sensitized solar cells, Nano Today 6 (2011) 91–109.
[29] M. Guo, P. Diao, Y.-J. Ren, F. Meng, H. Tian, S.-M. Cai, Photoelectrochemical studies of nanocrystalline TiO_2 co-sensitized by novel cyanine dyes, Solar Energy Materials and Solar Cells 88 (2005) 23–35.
[30] E. Galoppini, Linkers for anchoring sensitisers to semiconductor nanoparticles, Coordination Chemistry Reviews 248 (2004) 1283–1297.